Catalysis Letters, Vol. 113, Nos. 3–4, February 2007(© 2007)
DOI: 10.1007/s10562-007-9014-z

C_2H_2-SCR of NO over HZSM-5 affected by intracrystalline diffusion of NO_x

Xinping Wang,* Hongliang Yang, Qing Yu and Shixin Zhang

State Key Laboratory of Fine Chemicals, Dalian University of Technology, 288 #, Linggong Road 2, Dalian 116024, China

Received 5 November 2006; accepted 21 December 2006

The influence of particle size of HZSM-5 zeolite on selective catalytic reduction of NO by acetylene (C_2H_2-SCR) was investigated. The zeolite with nano-particle behaved considerable higher activity than the micro-particle one for the reaction. It was revealed that the large difference in the activity for the C_2H_2-SCR of NO arising from the particle size of zeolite was not caused by limited intracrystalline diffusion of the reductant, but that of NO_2, which was strongly supported by the adsorption results obtained over the zeolites.

KEY WORDS: nitrogen oxides; diffusion; SCR; acetylene; HZSM-5; crystal size.

1. Introduction

The selective catalytic reduction of NO with hydrocarbons (HC-SCR) in excess oxygen has received much attention recently because of its potential application to mobile lean-burn engines [1–4]. Since Cu-ZSM-5 was found to be capable of catalyzing the reduction of nitric oxide by hydrocarbons in the presence of excess oxygen [5,6], zeolite-based catalysts have been intensively investigated. For the HC-SCR of NO over this type of catalysts, one possible problem would be a limitation of catalytic reaction by intracrystalline diffusion [7,8]. Ogura and co-workers [9,10] found that the activity of In/HZSM-5 catalyst for CH_4-SCR of NO_2 decreased with the zeolite crystal size increasing. They attributed the dependence of catalytic activity on the zeolite particle size to the diffusion limitation of NO_2 caused by InO^+ sites that were formed in the channels of the zeolite. Shichi and co-workers investigated the influence of hydrocarbon molecular size on the activity of Cu-MFI zeolite for HC-SCR [11,12]. They found that when branched hydrocarbons such as 2, 2-dimethylbutane or i-octane were used as reducing agent, the reaction rate over the zeolite considerably depended on the zeolite crystal size. However, it was not observed when straight chain paraffines such as *n*-hexane or *n*-octane were used instead. A geometry-limited diffusion model in respect of the reductant was proposed by the authors to explain the kinetic difference caused by the zeolite size. Interestingly, a new concept of adsorption-controlled diffusion proposed by Shichi *et al*. [8,13] could reasonably explain the dependence of activity of the Cu-MFI catalyst for C_2H_4–, C_3H_6-SCR of NO upon the zeolite crystal size. Thus the HC-SCR of NO and/or NO_2 over the zeolite based catalysts in some cases was possibly retarded by the reductant intracrystalline diffusion over the zeolites, which were associated with large molecular size or strong adsorption affinity of the reductant to zeolite. However, we found that the activity of HZSM-5 zeolite towards NO oxidation to NO_2 as well as the selective catalytic reduction of NO by acetylene was also significantly affected by the crystal size of the zeolite. In this work, we investigate the activity of HZSM-5 for C_2H_2-SCR of NO influenced by the NO_2 intracrystalline diffusion.

*To whom correspondence should be addressed.
E-mail: dllgwxp@dlut.edu.cn

2. Experimental

2.1. Character of HZSM-5 samples

Two HZSM-5 samples characterized by XRD (figure 1) were used as catalyst for the C_2H_2-SCR of NO. The particle size of the samples was obviously different from each other (figure 2), but the Si/Al ratio of them was nearly identical (table 1). The HZSM-5 and NaZSM-5 zeolite with micro-particle was purchased from Nankai University (marked as HZSM-5(M) and NaZSM-5(M)), and the one with nano-particle was synthesized hydrothermally (marked as HZSM-5(N)).

2.2. Characterization of the zeolites

The temperature programmed desorption of ammonia (NH_3-TPD) over the samples was conducted on a conventional setup equipped with a thermal conductivity detector (TCD). The sample (0.1 g) was first pretreated in He at 550 °C for 30 min, then cooled to

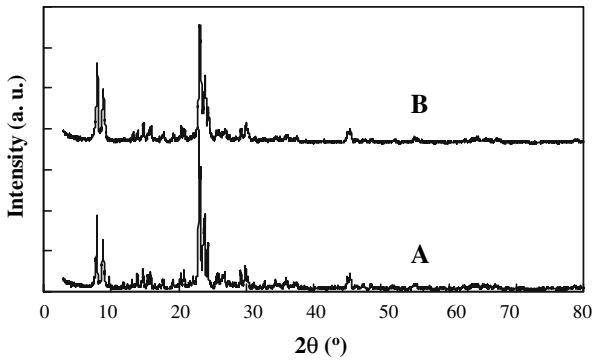

Figure 1. XRD patterns of HZSM-5 zeolites (A): HZSM-5(M), (B): HZSM-5(N).

Table 1
HZSM-5 zeolites used in the present study

Sample	Average diameter[a]	Content represented as oxides (%)[b]		
	(μm)	Na_2O	Al_2O_3	SiO_2
HZSM-5(M)	~ 1	–	5.98	92.4
HZSM-5(N)	~ 0.15	0.284	5.43	93.7

[a] Statistically calculated from SEM in large image region.
[b] Analyzed by X-ray fluorescence method.

100 °C and saturated with NH_3 until equilibrium. It was then flushed with He again until the baseline of the integrator was stable. Then the NH_3-TPD profile was recorded from 100 to 550 °C under a constant He flow of 30 mL·min^{-1} at temperature ramp of 10 °C·min^{-1}.

The adsorption experiment of acetylene on the catalyst was performed at 80 °C in a quartz reactor connected to a GC on-line. The zeolite sample (0.2 g) was pretreated on-line in N_2 at 500 °C for 1 h, and then cooled down to 80 °C for adsorption. By turning a four-way crossover valve, 2254 ppm of C_2H_2 in N_2 was passed through the sample at a flow rate of 30 mL·min^{-1}, during which the adsorbate in the outlet was analyzed constantly until reaching saturation adsorption. After that the sample was purged with N_2 at a flow rate of 30 mL·min^{-1} for 1 h, then the C_2H_2-TPD was recorded from 80 to 500 °C at temperature ramp rate of 10 °C·min^{-1}. For comparison, C_3H_6-TPD over 0.1 g of sample was also recorded in a similar procedure.

NO_2 adsorption over the samples was measured on a flowing system equipped with an electro-chemical NO_x analyzer (ACY301-B). After pretreated on-line in a quartz cell at 550 °C for 1 h in N_2 flow, cooled down to 40 °C, the sample (0.2 g) was exposed to a gas mixture containing 200 ppm of NO_2 in N_2 with a flow rate of 100 mL·min^{-1} until saturation adsorption. *In situ* FTIR spectra were recorded during the NO_2 adsorption in a quartz IR cell equipped with CaF_2 windows on Nicolet 360 FTIR spectrophotometer, by accumulating 32 scans at a resolution of 2 cm^{-1}. Zeolite self-supporting wafer was first activated in situ at 500 °C in N_2 flow, before the background spectrum (S_c) was recorded. Then the nitrous species formed over the zeolite was constantly measured while the sample exposing to the gas mixture of 1000 ppm of NO_2 in N_2 at 40 °C. Absorption arising from gas phase molecules in the cell on the pathway of infrared laser (S_g) was subtracted together with the S_c in the given IR spectra.

2.3. Activity evaluation

The selective catalytic reduction of NO by acetylene reaction was carried out in a quartz reactor (i.d. 4 mm) at atmospheric pressure. A mixture of 1600 ppm NO, 800 ppm C_2H_2, 10% O_2 in He with a total flow rate of 50 mL·min^{-1} was fed through 0.2 g catalyst ($GHSV \approx 8000$ h^{-1}). NO conversion was calculated from the amount of produced N_2 that was analyzed by gas chromatograph (HP 6890) with a capillary column (HP-PLOT/zeolite 30 m × 0.32 mm × 12μm).

The activity of the zeolites for NO oxidation to NO_2 was evaluated by passing 200 ppm of NO and 10% of O_2 in N_2 (100 mL·min^{-1}) at desired temperatures over the zeolite sample (0.2 g). Both produced NO_2 and unreacted NO were analyzed by NO_x analyzer. All reaction data were taken at steady state (that was generally reached in 40 min at each temperature).

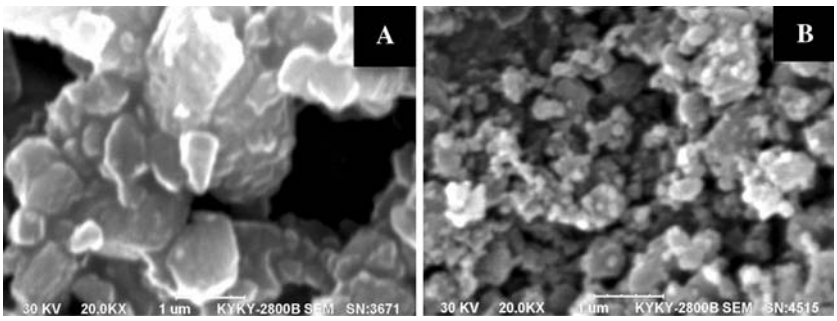

Figure 2. SEM images of A (HZSM-5(M)) and B (HZSM-5(N)) acquired on KYKY-2800B scanning electron microscope.

3. Results

3.1. Comparison in the activity for the C_2H_2-SCR of NO

Figure 3 shows the catalytic performance of HZSM-5(M) and HZSM-5(N) in the C_2H_2-SCR of NO. The HZSM-5(N) displayed a considerably higher NO conversion to N_2 at each reaction temperature compared with the HZSM-5(M), although the two zeolites have the identical MFI topological structure, as indicated by their XRD (figure 1). Furthermore, a great difference in the activity for NO oxidation was also observed over the two zeolites (figure 4). For example, the NO conversion to NO_2 was 29.6% over the HZSM-5(M) at 400 °C, while it increased to 34.2% when the HZSM-5(N) zeolite was used as catalyst in the same reaction condition. In our previous investigation, we have found that NO oxidation to NO_2 was a crucial step of C_2H_2-SCR of NO over the zeolite-based catalyst and the both reactions were strongly affected by the acidity of the catalyst [14,15]. Contrary to the large catalytic activity of HZSM-5(M), NaZSM-5(M) behaved nearly inert as catalyst in the C_2H_2-SCR of NO and in NO oxidation reaction for the two reactions (not shown), which indicates that protons in the zeolite play an important role in the two reactions [16]. To have an insight into the cause of the difference in the activity between the two HZSM-5 zeolites, the acidity of zeolites was characterized by NH_3-TPD (figure 5) and FTIR spectroscopy (figure 6). Obviously, the HZSM-5 zeolite with microparticle has more population of acid sites both with weak and strong acidity, corresponding to its larger ammonia desorption peaks at about 250 and 450 °C compared with the HZSM-5 zeolite with nano-particle. FTIR spectra of the zeolite self-supporting wafers also proved this result. Comparing with the HZSM-5(N), the HZSM-5(M) had significant larger absorption band at 3600 cm^{-1} due to Brönsted acid hydroxyl groups [17,18].

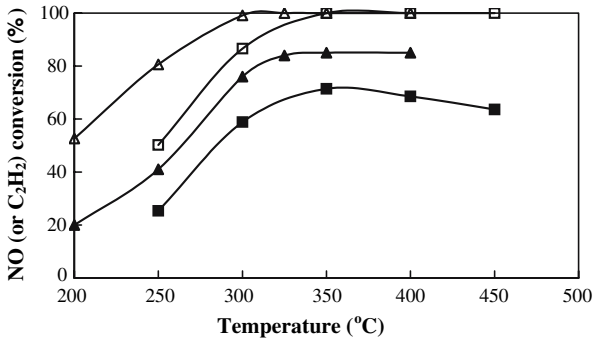

Figure 3. NO conversion to N_2 (closed symbols) and C_2H_2 conversion (open symbols) as a function of reaction temperature over HZSM-5(M) (■, □), and HZSM-5(N) (▲, Δ) at the reaction condition of 1600 ppm NO, 800 ppm C_2H_2, 10% O_2 in He, 0.2 g catalysts, 50 mL·min^{-1}.

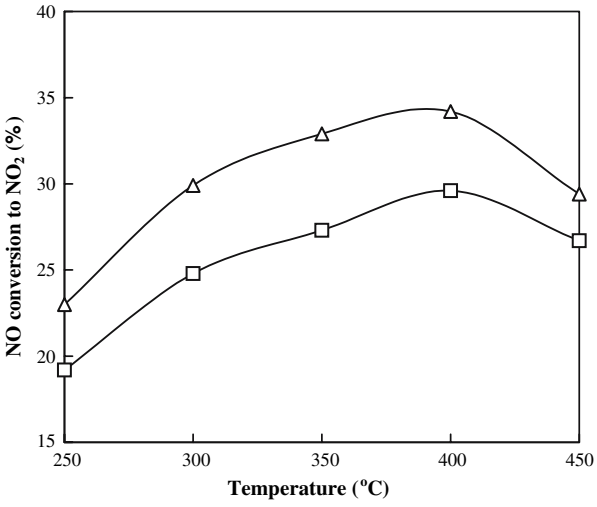

Figure 4. Catalytic activity of HZSM-5(M) (□) and HZSM-5(N) (Δ) for oxidation of NO with O_2. (Reaction conditions: 200 ppm of NO, 10% of O_2 in He, with a total flow rate of 100 mL·min^{-1} over 0.2 g catalyst).

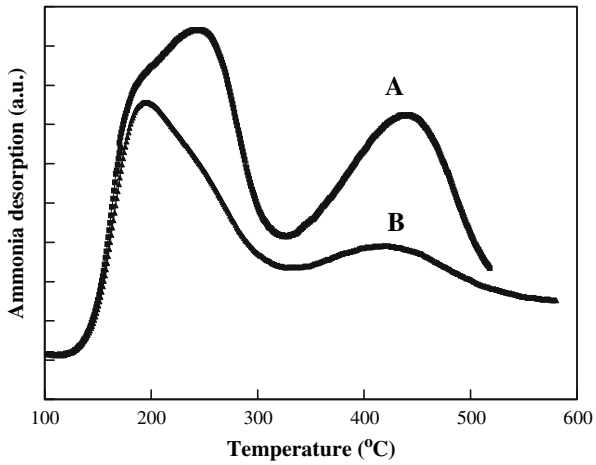

Figure 5. NH_3-TPD profiles of HZSM-5(M) (A); HZSM-5(N) (B).

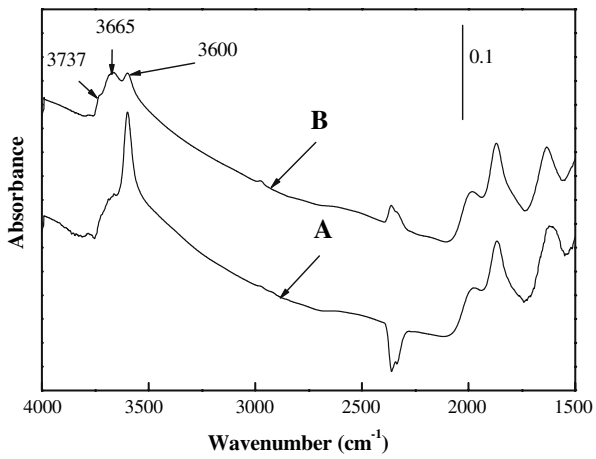

Figure 6. IR spectra of HZSM-5(M) (A) and HZSM-5(N) (B) recorded at 40 °C after treatment in N_2 at 500 °C for 30 min.

For the two zeolites, same scale of IR absorption in intensity of the bands both at 3737 cm^{-1} due to terminal silanol groups and at 3665 cm^{-1} due to hydroxyl groups attached to extra framework alumina [19] were observed. The results indicated that the zeolites had about same amount of the two kinds of hydroxyl groups. Thus, as the HZSM-5(M) has substantial larger population of acid sites than that of HZSM-5(N), one may expect that HZSM-5(M) would give higher activity for NO oxidation to NO_2 and for NO reduction to N_2 compared with the latter, if the reactions were not affected by intracrystalline diffusion for the zeolites. However, as mentioned above, just opposite results were observed. It implies that the reactions were retarded by the intracrystalline diffusion of the reactants when HZSM-5 zeolite was used as catalyst for the reactions.

3.2. Adsorption of C_2H_2 on the zeolites

Figure 7 shows variation of C_2H_2 concentration in the outlet during C_2H_2 adsorption on the zeolites at 80 °C. The curves obtained over the two zeolites were nearly superposable. It indicates that the adsorption of C_2H_2 over the two zeolites have the same adsorption rate during the adsorption process. Therefore, we conclude that the C_2H_2-SCR of NO over HZSM-5 zeolite was not influenced by intracrystalline diffusion of the reductant.

3.3. Adsorption of NO_2 on the zeolites

The performance of the two HZSM-5 zeolites for NO_2 adsorption at 40 °C was different from each other, which was contrary to that of C_2H_2 adsorption. The HZSM-5(M) behaved a NO_2 adsorption curve with lower slope compared with that of HZSM-5(N) (figure 8). The relative ratio of the slope for HZSM-5(M) and HZSM-5(N) was 0.74:1, indicating that the rate of

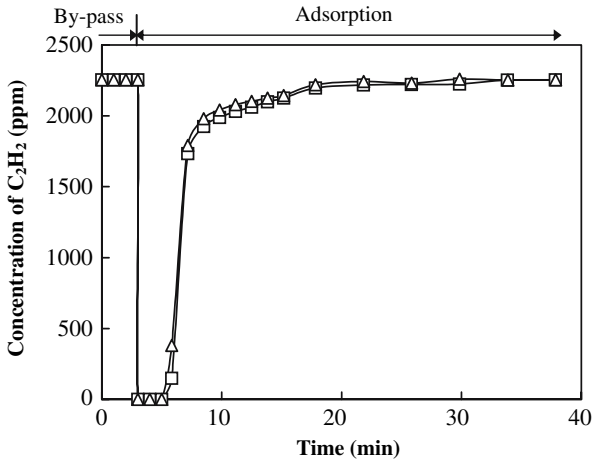

Figure 7. Time dependence of C_2H_2 concentration upon exposing the HZSM-5(M) (□), HZSM-5(N) (Δ) to 2254 ppm of C_2H_2 in N_2 at 80 °C.

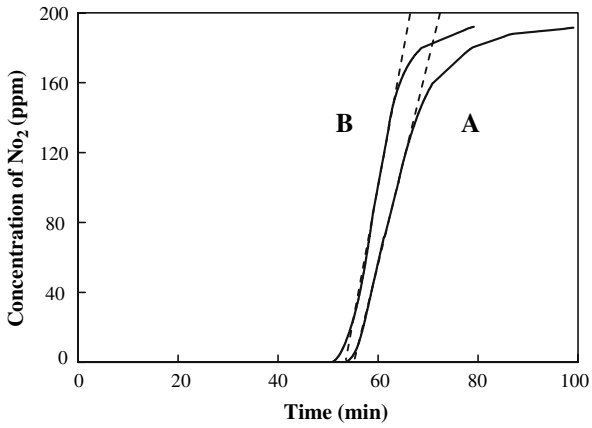

Figure 8. The NO_2 concentration in the effluent as a function of adsorption time over the HZSM-5(M) (A) and HZSM-5(N) (B) in 200 ppm NO_2 in N_2 at 40 °C.

NO_2 adsorption over the HZSM-5 zeolites at the temperature was a function of crystal size of the zeolites. The results were supported by IR spectra of nitrous species that were formed during NO_2 adsorption on the zeolites. As shown in figure 9, the increase of the nitrous species formed on HZSM-5(M) characterized by the IR spectra was considerably slower than that of HZSM-5(N) when the samples were exposed to 1000 ppm of NO_2 in N_2. For instance, the band at 1620 cm^{-1} due to bridging nitrates [20–22] retained its intensity after 1 min for NO_2 adsorption on HZSM-5(N), while that on HZSM-5(M) still obviously increased. Over HZSM-5(N), the band at 1309 cm^{-1} due to monodentate nitrates [23–25] appeared in 1 min and reached its maximum intensity in 25 min, while on HZSM-5(M), the same band appeared in 5 min upon NO_2 adsorption, and it reached the maximum intensity in 30 min. Obviously, the IR spectra concerning the NO_2 adsorption also suggest that the diffusion of NO_2 was easier over small crystal than over large ones, which was consistent with the result of figure 8 perfectly.

4. Discussion

As mentioned above, the less population of acid sites and slightly larger Si/Al ratio of HZSM-5(N) would negatively affect the activity of the zeolite for C_2H_2-SCR of NO as well as for the NO oxidation to NO_2. Thus, the higher activity of HZSM-5(N) for C_2H_2-SCR of NO could be attributed to its small particle size that may make the intracrystalline diffusion of the reactants easier. No evidence could be obtained to the speculation that there exists acetylene diffusion limitation over the HZSM-5 zeolites. It can be comprehended as follows: (1) Acetylene is small linear molecule, geometry limited diffusion was impossible for the reductant over the zeolite. (2) Acetylene has rather less tendency to be

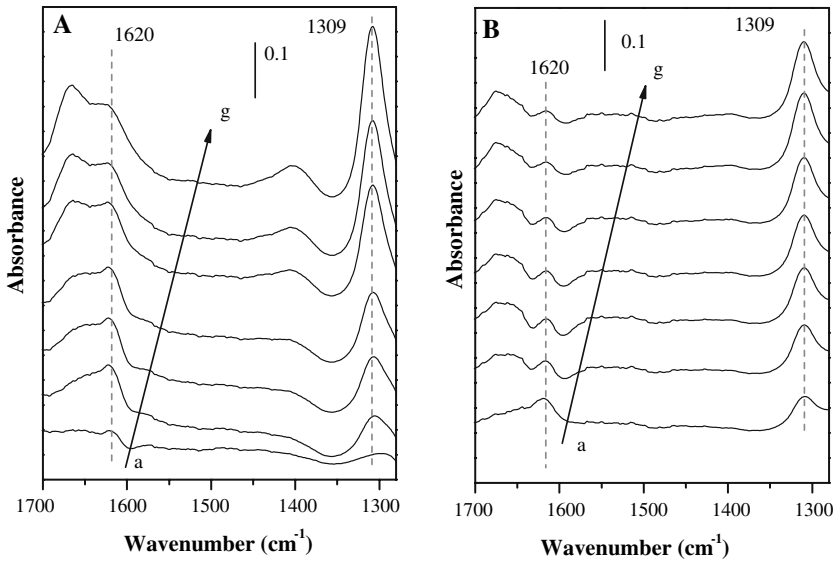

Figure 9. FTIR spectra of nitrous species formed on HZSM-5(M) (A) and HZSM-5(N) (B) during NO_2 adsorption : (a) 1 min, (b) 5 min, (c) 10 min, (d) 15 min, (e) 20 min, (f) 25 min, (g) 30 min.

adsorbed by the zeolites than propene (figure 10), which should be noted herein, although it has the triple bond. So the adsorption controlled diffusion would hardly work as well for acetylene diffusion over the HZSM-5 zeolites.

On the other hand, diffusion limitation of NO_2 over the zeolites was observed (figures 8, 9), which explains the substantially larger activity of HZSM-5(N) than HZSM-5(M) for the NO oxidation to NO_2. As shown in figure 11, NO_2 can be adsorbed on HZSM-5 forming monodentate, bridging bidentate and chelating bidentate nitrate adsorption surface species [20]. Some of the nitrate species so strongly interacted with the zeolite that they could remain on the zeolite surface above 300 °C [16]. As a result, the strong adsorption of NO_2 in the channels of zeolite limited the intracrystalline diffusion of reactant molecules. Thus, it was well interpreted that the HZSM-5 zeolite with nano-particle behaved higher activity than the one with micro-particle for NO oxidation to NO_2 and for the C_2H_2-SCR of NO.

5. Conclusion

No limited intracrystalline diffusion of acetylene could be observed over the HZSM-5 zeolites. However, NO_2 diffusion in the zeolite channels was limited by part of strong adsorption of them on the surface of the

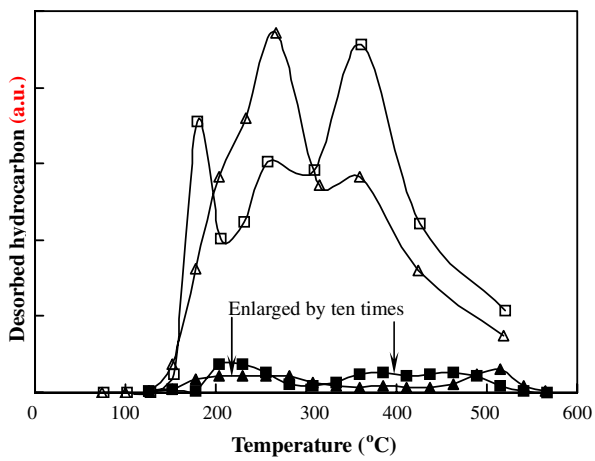

Figure 10. TPD of C_2H_2 (■, ▲) and C_3H_6 (□, Δ) over HZSM-5(M) (■, □) and HZSM-5(N) (▲, Δ) in N_2. The signal intensity in C_2H_2-TPD was enlarged by 10 times. The zeolite samples used in C_3H_6-TPD were half of those used in C_2H_2-TPD.

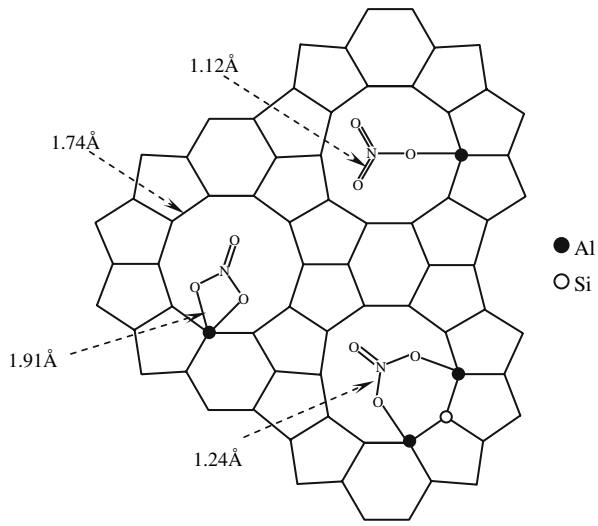

Figure 11. Schematic representation of NO_2 adsorbed in the channels of HZSM-5.

zeolite, which was the reason why the activity of the HZSM-5 zeolite for C_2H_2-SCR of NO and for NO oxidation was a function of the particle size of the zeolite.

Acknowledgments

We thank the National Natural Science Foundation of China for financial support (Grant No.20677006).

References

[1] M.D. Fokema and J.Y. Ying, Catal. Rev. 43(1&2) (2001) 1.
[2] R. Burch, J.P. Breen and F.C. Meunier, Appl. Catal. B 39 (2002) 283.
[3] H. Chen, Q. Sun, B. Wen, Y. Yeom, E. Weitz and W.M.H. Sachtler, Catal. Today 96 (2004) 1.
[4] M.A. Gómez-García, V. Pitchon and A. Kiennemann, Environ. Int. 31 (2005) 445.
[5] M. Iwamoto, H. Yahiro, S. Shundo and N. Miaunov, Shokubai 32 (1990) 430.
[6] W. Held, A. Konig, T. Ritcher and L. Puppe, SAE 900469 (1990).
[7] T. Tabata and H. Ohtsuka, Catal. Lett. 48 (1997) 203.
[8] A. Shichi, A. Satsuma and T. Hattori, Catal. Today 93–95 (2004) 777.
[9] M. Ogura and E. Kikuchi, Chem. Lett. (1996) 1017.
[10] M. Ogura, T. Ohsaki and E. Kikuchi, Micro. Meso. Mater. 21 (1998) 533.
[11] A. Shichi, A. Satsuma and T. Hattori, Appl. Catal. B 30 (2001) 25.
[12] A. Shichi, A. Satsuma and T. Hattori, Appl. Catal. A 207 (2001) 315.
[13] A. Shichi, A. Satsuma, K. Katagi and T. Hattori, Appl. Catal. B 24 (2000) 97.
[14] X. Wang, Y. Xu, S. Yu and C. Wang, Catal. Lett. 103 (2005) 101.
[15] X. Wang, S. Yu, H. Yang and S. Zhang, Appl. Catal. B 71 (2006) 246.
[16] Q. Yu, X. Wang, N. Xing, H. Yang and S. Zhang, J. Catal. 245 (2007) 124).
[17] K. Hadjiivanov, J. Saussey, J.L. Freysz and J.C. Lavalley, Catal. Lett. 52 (1998) 103.
[18] H.H. Ingelsten, D. Zhao, A. Palmqvist and M. Skoglundh, J. Catal. 232 (2005) 68.
[19] G. Li, S.C. Larsen and V.H. Grassian, Catal. Lett. 103 (2005) 23.
[20] C. Sedlmair, K. Seshan, A. Jentys and J.A. Lercher, J. Catal. 214 (2003) 308.
[21] G. Li, S.C. Larsen and V.H. Grassian, J. Mol. Catal. A 227 (2005) 25.
[22] Y. Yu, H. He, Q. Feng, H. Gao and X. Yang, Appl.Catal. B 49 (2004) 159.
[23] K. Shimizu, J. Shibata, H. Yoshida, A. Satsuma1 and T. Hattori, Appl. Catal. B 30 (2001) 151.
[24] H. He, C. Zhang and Y. Yu, Catal. Today 90 (2004) 191.
[25] M. Mihaylov, K. Hadjiivanov and D. Panayotov, Appl. Catal. B 51 (2004) 33.